

A wideband coherent terahertz spectroscopy system using optical rectification and electro-optic sampling

Ajay Nahata,^{a)} Aniruddha S. Weling, and Tony F. Heinz

Departments of Electrical Engineering and Physics, Columbia University, New York, New York 10027

(Received 23 May 1996; accepted for publication 7 August 1996)

We present a scheme for exploiting the nonresonant second-order nonlinearities in electro-optic media to extend the bandwidth of coherent spectroscopy in the far-infrared using ultrafast laser pulses. Using optical rectification and electro-optic sampling in $\langle 110 \rangle$ ZnTe for the generation and coherent detection of freely propagating THz radiation, respectively, we have demonstrated spectral sensitivity beyond 3 THz. This was accomplished by achieving phase matching for both optical rectification and electro-optic sampling over a broad range of THz frequencies. © 1996 American Institute of Physics. [S0003-6951(96)03542-5]

In recent years, remarkable progress has been made in the development of spectroscopic capabilities for coherent terahertz (THz) measurements.^{1,2} A key ingredient in these advances is the development of broadband coherent sources and detectors of THz radiation. Much of the work reported to date relies on the use of photoconductive elements both as emitters and detectors.^{1,3} While these devices are highly optimized in many respects, there are fundamental limitations in their frequency response associated with the natural time constants for carrier dynamics.¹ The ready availability of laser pulses with durations of ~ 10 fs^{4,5} suggests the potential for extending the bandwidth of coherent spectroscopy to significantly higher frequencies. By using materials with an instantaneous optical response for both emission and detection, it may be possible to capture much of this enormous bandwidth. This suggests the use of materials with nonresonant second-order optical nonlinearities for these applications.

THz radiation may be produced in an electro-optic medium via difference-frequency mixing.⁶⁻⁹ The generation process may be regarded as the beating of various Fourier components of the driving optical spectrum to produce an optically rectified baseband pulse.¹⁰ Such a difference-frequency generation scheme is capable of producing electric fields with spectral content extending from dc¹¹ to the mid-infrared.¹² For detection of the THz electric field wave form, this mixing process can be reversed in an electro-optic medium. Valdmanis *et al.*¹³ have shown that electro-optic sampling is a sensitive probe of localized electric fields in transmission lines and high-speed circuits. This approach has recently been extended to the coherent detection of freely propagating THz radiation.^{14,15} In this letter, we describe a wideband coherent THz spectroscopy system using optical rectification for the generation of THz radiation and electro-optic sampling for the coherent detection of this radiation, both in $\langle 110 \rangle$ ZnTe. The electro-optic sampling measurement is performed in a transmission geometry. This geometry allows for the copropagation of the THz and probe beams over an extended path length while maintaining ultrashort response times. An important consideration which we address here is the use of phase matching to allow for greater interaction between the optical and THz pulses in the

nonlinear medium in order to enhance the efficiency of both the generation and detection processes.

Both broadband optical rectification and electro-optic sampling have been demonstrated in thin $\chi^{(2)}$ media.^{14,16} In order to enhance the sensitivity, longer interaction lengths are desirable, necessitating appropriate consideration of phase matching constraints.¹⁰ The phase matching condition for the optical rectification process (collinear difference frequency mixing) is given by

$$\Delta k = (\omega_{\text{opt}} + \omega_{\text{THz}}) - k(\omega_{\text{opt}}) - k(\omega_{\text{THz}}) = 0, \quad (1)$$

where ω_{opt} and ω_{THz} are the optical and THz frequencies, respectively, and ω_{opt} and $(\omega_{\text{opt}} + \omega_{\text{THz}})$ lie within the spectrum of the optical pulse. An equivalent equation can be written for electro-optic sampling. If we neglect dispersion in the optical spectral range, we can express the coherence length $l_c (= \pi/\Delta k)$ as

$$l_c = \frac{\pi c}{\omega_{\text{THz}} |n_{\text{opt}} - n_{\text{THz}}|}. \quad (2)$$

Here, c is the speed of light and n_{opt} and n_{THz} are the optical and THz refractive indexes, respectively. In inorganic nonlinear optical crystals, the difference between the optical and THz refractive indexes tends to be large, because of the contribution of low lying phonon resonances to the THz refractive index. The optical refractive indexes of ZnTe may be obtained from the equation¹⁷

$$n^2 = 4.27 + 3.01\lambda^2/(\lambda^2 - 0.142), \quad (3)$$

where λ is the optical wavelength in μm . The far-infrared (FIR) refractive indexes may be obtained from¹⁸

$$n^2 = (289.27 - 6f_{\text{THz}}^2)/(29.16 - f_{\text{THz}}^2), \quad (4)$$

where $f_{\text{THz}} (= \omega_{\text{THz}}/2\pi)$ is in THz. Using Eq. (3), the optical refractive index of ZnTe at 800 nm is 2.85. Figure 1 shows the coherence length as a function of FIR frequency, f_{THz} , calculated using Eq. (2).

Birefringence has been employed to achieve long coherence lengths in optical rectification experiments.¹⁰ However, the large refractive index difference between the optical and FIR results in a narrow phase matching bandwidth. Angle tuning in a noncollinear beam geometry has also been shown

^{a)}Electronic mail: an23@columbia.edu

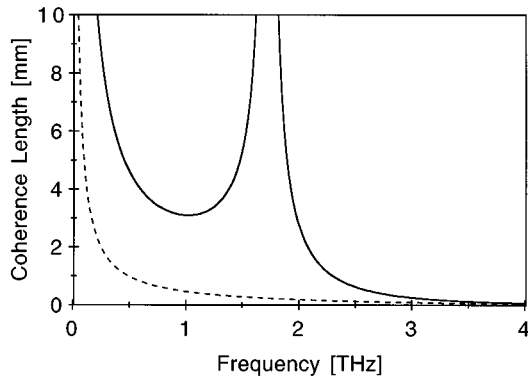


FIG. 1. Coherence length vs THz frequency for ZnTe using optical excitation at 800 nm. The dotted line, calculated using Eq. (2), neglects the dispersion at optical frequencies. The solid line, calculated using Eq. (6), includes the effects of dispersion at optical frequencies.

to increase interaction lengths.¹³ However, the requisite angle is often greater than the critical angle, requiring specialized sample preparation. Additionally, this method may degrade the time resolution. We demonstrate that dispersion in the optical refractive index may be used to obtain collinear, noncritical phase matching over a broad bandwidth in the THz. For a medium with dispersion at optical frequencies, the phase matching condition of Eq. (1) may be rewritten as

$$\frac{k(\omega_{\text{THz}})}{\omega_{\text{THz}}} \approx \left(\frac{\partial k}{\partial \omega} \right)_{\text{opt}}. \quad (5)$$

This relation implies that phase matching is achieved when the phase of the THz wave travels at the velocity of the optical pulse envelope (i.e., the optical group velocity, v_g). The corresponding coherence length for difference frequency mixing and electro-optic sampling is now

$$l_c = \frac{\pi c}{\omega_{\text{THz}} \left| n_{\text{opt}} - \lambda_{\text{opt}} \frac{dn_{\text{opt}}}{d\lambda} \Big|_{\lambda_{\text{opt}} - n_{\text{THz}}} \right|}. \quad (6)$$

Using the refractive index data in Eq. (3), we find that the effective optical refractive index, $N_{\text{eff}} = n_{\text{opt}} - \lambda_{\text{opt}}(dn_{\text{opt}}/d\lambda)$ at 800 nm is 3.22. Using Eq. (6), the modified coherence length versus FIR frequency, f_{THz} , for ZnTe is also shown in Fig. 1. The data indicate that sufficient group velocity dispersion exists within ZnTe to obtain phase matching beyond $f_{\text{THz}} \sim 2$ THz. The coherence length decreases because of dispersion in the THz refractive index, but remains large over a wide range of frequencies, as demonstrated below.

The experimental setup for generating and detecting THz radiation is shown in Fig. 2. A mode-locked Ti:sapphire laser producing 130 fs pulses at 800 nm with a 76 MHz repetition rate was used to generate and detect the FIR pulses. A 2 mm diam pump beam, with an average power of 350 mW, was chopped and used to drive a 0.9 mm thick $\langle 110 \rangle$ ZnTe emitter at normal incidence. The pump beam was polarized at an angle of 60° to the $\langle 110 \rangle$ crystallographic direction in order to maximize the nonlinear response.⁸

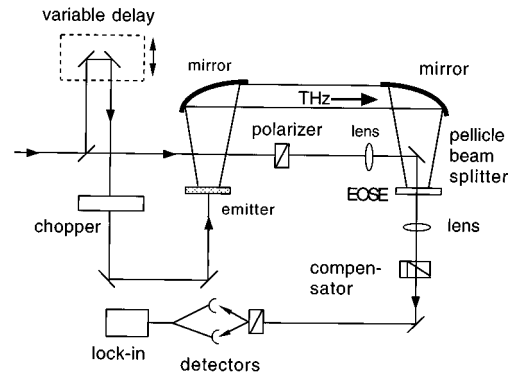


FIG. 2. Schematic drawing of the experimental setup used to detect freely propagating THz radiation. $\langle 110 \rangle$ ZnTe was used to generate THz radiation by optical rectification and detect THz radiation by electro-optic sampling.

The THz electromagnetic transient produced by optical rectification in the ZnTe crystal was imaged into an identical ZnTe crystal [hereafter referred to as the electro-optic sampling element (EOSE)] using two off-axis paraboloidal mirrors. A Teflon filter was used to block the unwanted optical pump beam and pass the FIR. The THz field was polarized parallel to the $\langle 001 \rangle$ axis of the $\langle 110 \rangle$ ZnTe EOSE. The total separation between the emitter and detector was 50 cm. A pellicle beamsplitter was interposed in the THz beam line to allow for copropagation of the optical probe and THz beams through the EOSE. The 5 μm thick pellicle membrane had negligible effect on the THz wave form. A probe beam was optically biased at its quarter wave point by a Soleil-Babinet compensator and a crossed polarizer arrangement with differential detection was used in order to improve the sensitivity.¹³

The temporal wave form of the measured THz electric field is shown in Fig. 3. The full width at half-maximum (FWHM) pulsewidth is ~ 270 fs. The small oscillations after the main peak are believed to be due, in part, to the free induction decay of the ambient water vapor excited by passage of the THz beam.¹⁹ We note that in this geometry, both beams undergo multiple internal reflections within the EOSE. In the current experiment, these were excluded by appropriate narrowing of the temporal scan window. If desired, however, these reflections can be significantly reduced

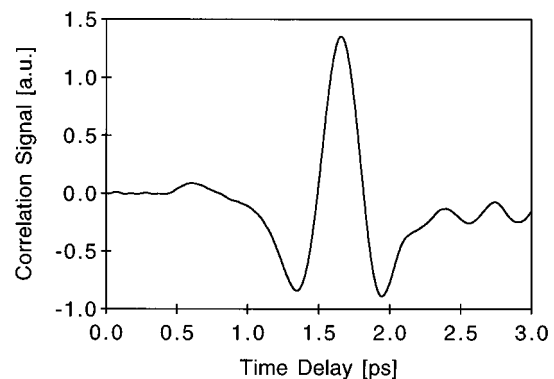


FIG. 3. Temporal wave form detected by electro-optic sampling. The FWHM pulse width is 270 fs.

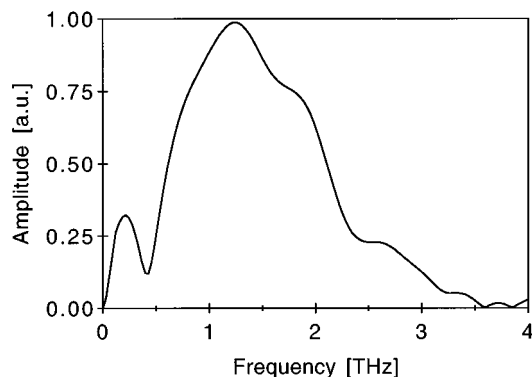


FIG. 4. Amplitude spectrum of the temporal wave form shown in Fig. 3.

by bonding the ZnTe to an appropriate optically transparent, high index substrate.

The amplitude spectrum of the temporal wave form is shown in Fig. 4, demonstrating the wide band capability of the system. A 3 dB reduction in the amplitude spectrum occurs at ~ 2 THz. We compare this result to the phase matching characteristics shown in Fig. 1. From this figure, we find that the maximum frequency for obtaining a coherence length exceeding the thickness of the ZnTe crystals (0.9 mm) is ~ 2.5 THz. Thus, we would expect a rolloff in sensitivity for higher frequencies, due to the reduced interaction length. This is reasonable agreement with the amplitude spectrum properties. In addition to the limitations imposed by phase matching, the absorption caused by the dominant low frequency resonance in ZnTe at 5.4 THz¹⁸ is expected to attenuate the high frequency components of the THz radiation.

For our ZnTe EOSE and shot-noise limited differential detection, photomodulation as small as $5 \times 10^{-8} / \sqrt{\text{Hz}}$ may be detected [corresponding to a minimum detectable field of ~ 2 (mV/cm)/ $\sqrt{\text{Hz}}$]. The significant improvement in sensitivity of the EOSE as compared to the earlier results using poled polymers¹⁴ is largely due to the use of the phase matched transmission geometry which allows for greater interaction lengths. In practice, our sensitivity is lower by a factor of 100 and is believed to be due to excess laser noise. Modulation of the pump beam at significantly higher frequencies should reduce this noise.

In our current experimental arrangement, the coherence length decreases rapidly beyond 2 THz due to the dispersion in the FIR. It should be possible to increase this 3 dB detection frequency by using shorter wavelength optical radiation. This will increase N_{eff} , thereby shifting the coherence length curve to higher frequencies. A substantial improvement in the bandwidth capability and system sensitivity may also be expected by using materials with resonances lying at higher THz frequencies. Among inorganic media with comparable nonlinearities, ZnSe (lowest resonance at 6 THz) and GaAs (lowest resonance at 10 THz) are promising candidates. Or-

ganic crystals are also extremely promising for this application. Many of these materials exhibit optical nonlinearities that are essentially electronic in nature, offering the possibility of ultra-wideband generation and detection.

In conclusion, we have demonstrated a wideband THz spectroscopy system with useful spectral information beyond 3 THz. Coherent FIR radiation is generated via optical rectification and detected via electro-optic sampling in $\langle 110 \rangle$ ZnTe. We have shown that the dispersion at optical frequencies in ZnTe may be used to significantly increase the coherence lengths for these two processes over a broad range of frequencies in the FIR. With the use of electro-optic materials exhibiting lower dispersion in the FIR, it should be possible to extend the bandwidth capability of this system with enhanced detection sensitivity.

Note added in proof: After submission of this manuscript, Zhang and co-workers [Q. Wu, M. Litz, and X.-C. Zhang, Appl. Phys. Lett. **68**, 2924 (1996)] published related results using a GaAs emitter and ZnTe detector.

A.N. is grateful to David H. Auston for his continued guidance and encouragement. This research was supported by the Air Force Office of Scientific Research under Grant F49620-92-J-0036.

- ¹D. Grischkowsky, in *Frontiers in Nonlinear Optics*, edited by H. Walther, N. Koroteev, and M. O. Scully (Institute of Physics, Philadelphia, 1992), and references therein.
- ²M. van Exter and D. Grischkowsky, IEEE Trans. Microwave Theory Tech. **38**, 1684 (1990).
- ³D. H. Auston, K. P. Cheung, and P. R. Smith, Appl. Phys. Lett. **45**, 284 (1984); P. R. Smith, D. H. Auston, and M. C. Nuss, IEEE J. Quantum Electron. **24**, 255 (1988).
- ⁴F. Krausz, M. E. Fermann, T. Brabec, P. F. Curley, M. Hofer, M. H. Ober, C. Spielmann, E. Wintner, and A. J. Schmidt, IEEE J. Quantum Electron. **QE-28**, 2097 (1992).
- ⁵M. T. Asaki, C.-P. Huang, D. Garvey, J. Zhou, H. C. Kapteyn, and M. M. Murnane, Opt. Lett. **18**, 977 (1993).
- ⁶B. Hu, X.-C. Zhang, D. H. Auston, and P. R. Smith, Appl. Phys. Lett. **56**, 506 (1990).
- ⁷L. Xu, X.-C. Zhang, and D. H. Auston, Appl. Phys. Lett. **61**, 1784 (1992).
- ⁸A. Rice, Y. Jin, X. F. Ma, X.-C. Zhang, D. Bliss, J. Larkin, and M. Alexander, Appl. Phys. Lett. **64**, 1324 (1994).
- ⁹T. Yajima and N. Takeuchi, Jpn. J. Appl. Phys. **9**, 1361 (1970).
- ¹⁰Y.-R. Shen, Prog. Quantum Electron. **4**, 207 (1976).
- ¹¹J. F. Ward, Phys. Rev. **143**, 569 (1966).
- ¹²A. Bonalet, M. Joffre, J. L. Martin, and A. Migus, Appl. Phys. Lett. **67**, 2907 (1995).
- ¹³J. A. Valdmanis, G. Mourou, and C. W. Gabel, Appl. Phys. Lett. **41**, 211 (1982); J. A. Valdmanis and G. Mourou, IEEE J. Quantum Electron. **22**, 69 (1986).
- ¹⁴A. Nahata, D. H. Auston, T. F. Heinz, and C. Wu, Appl. Phys. Lett. **68**, 150 (1996).
- ¹⁵Q. Wu and X.-C. Zhang, Appl. Phys. Lett. **67**, 3523 (1995); Q. Wu and X.-C. Zhang, Appl. Phys. Lett. **68**, 1604 (1996).
- ¹⁶A. Nahata, D. H. Auston, C. Wu, and J. T. Yardley, Appl. Phys. Lett. **67**, 1358 (1995).
- ¹⁷D. T. F. Marple, J. Appl. Phys. **25**, 539 (1964).
- ¹⁸T. Hattori, Y. Homma, A. Mitsuishi, and M. Tacke, Opt. Commun. **7**, 229 (1973).
- ¹⁹M. van Exter, Ch. Fattinger, and D. Grischkowsky, Opt. Lett. **14**, 1128 (1989).